Journal of Science and Technology Research

Journal homepage: www.nipesjournals.org.ng

Buckling of Externally Pressurized Toroidal Vessels with Circular-Elliptical Cross-Section

N. Enoma, J. Madu*

Department of Mechanical Engineering, University of Benin, Benin City, Nigeria

Article Info	**Abstract**
	Buckling is a prominent failure mode of thin-walled structures, and its information is very crucial. This is readily available for a complete toroidal shell with circular cross-section - a traditional toroid - which has been well-researched through analytical and numerical approaches due to their relatively non-complicated cross-sectional profile. On the other hand, information about the buckling of non-conventional toroids is rare, owing to the associated difficulties in the analytical investigation approaches. Hence, numerical methods are nowadays usually employed for studies on these shell types. This is adopted in the present paper to investigate the buckling behaviour of a circular-elliptical toroidal shell under external pressure. The vessel consists of a top semi-circular toroidal segment that is joined tangentially to a bottom semi-elliptical segment at their equatorial circles of latitude within the inner and outer regions of the toroidal vessel. The results from the numerical model were validated through extreme cases with available data in the literature. It is shown that circular-elliptical toroidal vessels have a stable post-buckling behaviour and may be able to resist further load beyond the elastic bifurcation load. A parametric study was also conducted, revealing more insights into the buckling response of the vessel.

1. Introduction

Elastic shell theories and the geometry of toroidal shells are relatively complicated when compared with traditional shells used in engineering applications [1]. Closed toroidal shells are employed in space, nuclear and under-water fields, where buckling may be prevalent depending on the mode of loading. Some results for the buckling of toroidal shells of have been presented by [2], where focus was on toroids with elliptical cross-section subjected to internal pressure. The buckling response of liquid-filled barrel shells has been presented [3], while [4] examined the buckling behaviour of vessels supported by using two saddles. In [5], the comparison of numerical programs BOSOR 5 (which employed variational finite differences technique) [6] and INCA [7] for computing the buckling toroidal shells was carried out, where the two programs gave buckling pressures which agree within 6% for prolate elliptical toroids. [8] worked on the plastic buckling pressures of various internally pressurized toroidal shells of elliptical cross section. It noted that the buckling pressure was approximately equal to their elastic counterparts, when the major-to-minor axis ratio is equal to 2.5. The buckling performance of multi-segment pressure subjected to uniform hydrostatic pressure was discussed by [9], in which the experimental and numerical collapse pressure yielded similar results.

The present paper numerically analyses the buckling behaviour of a novel toroidal vessel with circular-elliptical cross-section under external pressure loading, including the buckling response of the vessel due to changes in the cross-sectional geometrical parameters. The sketch of the non-conventional toroidal vessel is shown in Figure 1 with the loading and geometrical parameters. The vessel consists of a top semi-circular toroidal segment that is joined tangentially to a bottom semi-elliptical segment at their equatorial circles of latitude (at D^o in the outer region and D^i in the inner region of the vessel). Consequently, the total height of the vessel is $a+b$, where a is the local radius and the local (horizontal) semi-axis of the semi-circular and semi-elliptic toroidal segments, respectively, and b is the local (vertical) semi-axis of the semi-elliptic segment. The toroidal mean radius of the vessel is denoted by A and the entire external surface of the vessel is subjected to a uniform pressure, which is denoted by a patch pressure load p in Figure 1.
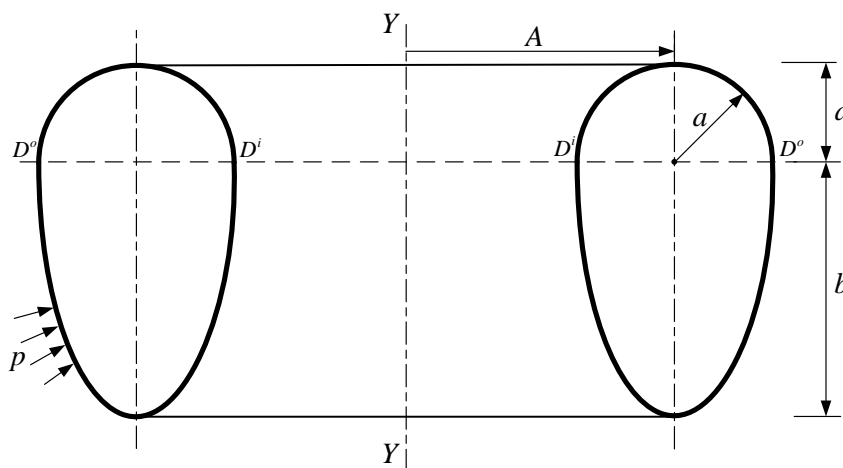

Figure1: Sketch of the cross-sectional view of a pressurised circular-elliptic toroidal vessel

2. Numerical modelling of the circular-elliptic toroid

The FE modelling of the circular-elliptic toroidal vessel specimens was done in ABAQUS using both the three-node quadratic axisymmetric thin shell element (SAX2) and four-node doubly curved thin shell element (S4R), in accordance with the modelling procedure and assumptions of [10]. The element-type that gives the smallest eigenvalues was adopted in the modified Riks algorithm [11], which was implemented in ABAQUS for nonlinear static equilibrium solutions of unstable problems. The Riks algorithm has been employed here to investigate the nonlinear load-deflection behaviour of toroids, since it can detect and go beyond limit points. The toroidal shell material is modelled as elastic steel with Young modulus $E = 210 \times 10^9 \, N/m^2$, and Poisson's ratio $\upsilon = 0.3$.

A preliminary mesh convergence study was conduction for each of the element types to establish the suitable mesh densities to be adopted. The following mesh densities were found to be appropriate for the toroidal models: an approximate global seeds size of 0.25 with a maximum deviation factor of 0.1 for the axisymmetric models (SAX2); and quad-dominated local seeds of approximate size 0.25 with a maximum deviation factor of 0.1 for the full models (S4R). Following the work of [10], the adopted boundary conditions leading to the lowest eigenvalues in this paper are presented in Table 1 for the axisymmetric models (SAX2) and the full models (S4R). As shown in the table, the nodes at the inner meeting circle of latitude are restrained translationally in the axial (meridional), and normal directions in the SAX2 models and all the nodes at the inner meeting circle of latitude are fully restrained translationally in the S4R models.

Table1: Boundary conditions in both models

SAX2 models			S4R models					
u_r	u_z	Φ_{rz}	u_x	u_y	u_z	Φ_x	Φ_y	Φ_z
0	0	$\neq 0$	0	0	0	$\neq 0$	$\neq 0$	$\neq 0$

2.1. Numerical example and validation

Eigenvalue analysis was initially conducted on an externally pressurised circular-elliptical toroidal vessel with $b/a = 4.0$, $A/a = 2.0$, $a/t = 200$, using both the SAX2 and S4R algorithms. The buckling plots of the first eigenmodes obtained from the two models are shown in Figure 2. The axisymmetric buckling mode from the SAX2 model is shown in a deformation scale of +4 in Figures 2(a), while the asymmetric bifurcation buckling mode (characterised by $n = 27$ circumferential waves) from the S4R model is shown in a deformation scale of +2 in Figures 2(b).
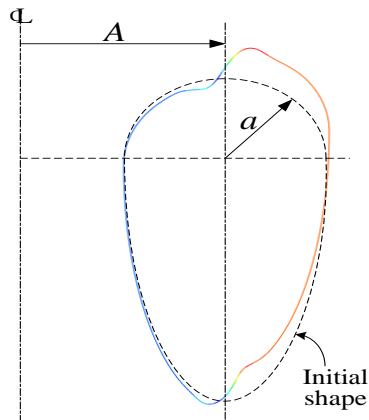

Figure 2 (a): SAX2 first axisymmetric buckling mode for a toroid with $b/a = 3.0$, $A/a = 2.0$, $a/t = 200$

Figure 2 (b): S4R first buckling mode for a toroid with $b/a = 3.0$, $A/a = 2.0$, $a/t = 200$, $n = 27$

The magnitude of each of the first buckling pressures obtained from the two approaches is given in Table 2. It is noticed that, for this example, the first eigenvalue obtained from the axisymmetric model (SAX2) is over three times larger than that from the full model (S4R). This is an indication

that the lowest buckling mode of the pressurised vessel is asymmetrical about the global axis $Y - Y$ of the vessel, as seen in Figure 2 (b). Hence, the critical buckling pressure of interest is $p_{cr} = 0.160 MPa$, (the first eigenvalue obtained from the S4R model for this case), as shown in Table 2.

Table 2: Comparison of buckling pressures from SAX2 and S4R shell models

b/a	A/a	a/t	$p(MPa)$		
			SAX2	S4R	p_{cr}
3.0	2.0	200	0.252	0.160	0.160

The critical buckling pressure was then used in the nonlinear static Riks analysis of the pressurised vessel. The program was set to terminate after 400 increments, and 0.4, 10⁻⁶ and 0.4 initial, minimum and maximum arc length increments. A typical load-deflection curve obtained for the toroidal vessel with $b/a = 3.0$, $A/a = 2.0$, $a/t = 200$ is shown in Figure 3, where the variation in the external pressure to critical buckling pressure ratio (p/p_{cr}) is plotted against the vertical displacement of the lowest circle of latitude (nadir) per shell thickness $(\Delta y/t)$.
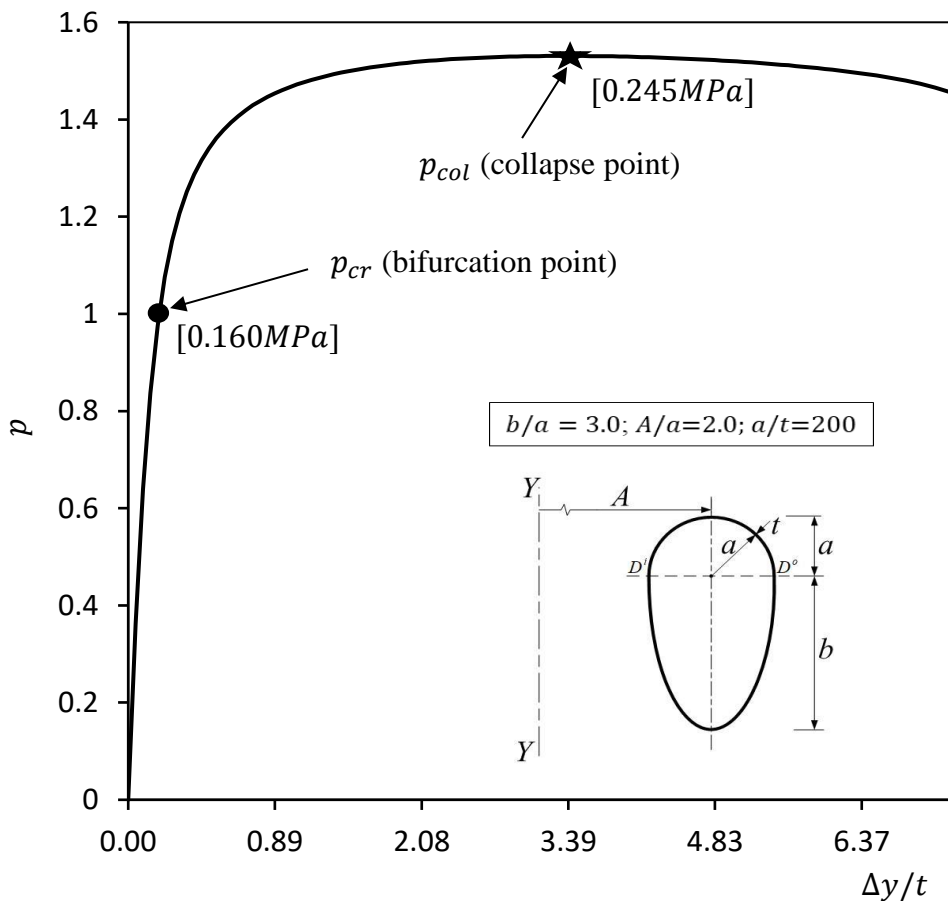

Figure 3: The plot of external pressure versus nadir deflection for a toroid with $b/a = 3.0$, $A/a = 2.0$, $a/t = 200$

As seen in Figure 3, the bifurcation buckling is initiated in the zone with the least stiffness mainly as a result of relatively large values of the principal radius of curvature r_1 spanning through a wide

spectrum of the meridional profile on the positive Gaussian side of the vessel where the failure started. The span of the meridional spectrum with large values of r_1 is a function of b/a ratio. In the meridional span under discussion, ϕ is around π and for $b/a \gg 1$, the angle ϕ changes very slowly as one move away from the equator of the semi-elliptical segment. This results in a wider meridional span with large values of r_1. The value of b/a from which the present toroidal vessel starts to fail in a non-symmetric mode by bifurcation buckling.

To be able to validate the results, an extreme case of the present circular-elliptical toroidal vessel, where $b = a$ is used. Hence, the vessel reduces to a circular toroid, which has readily available results for buckling in the literature. For ease of comparison, linear eigenvalue analyses were conducted on a set of circular toroids with geometrical parameters adopted from [2], in which the buckling pressures were calculated using the French finite element program, INCA. The critical buckling results obtained from the present FEM approach are compared with those from the studies by Sobel & Flügge [12], Wang & Zhang [13], and Galletly & Błachut [2] in Table 3. It could be seen that the obtained numerical results in the last column are almost identical to the results obtained from the French finite element program, INCA by Galletly & Błachut, and also compare very well with the results from the studies by Sobel & Flügge, Wang & Zhang.

Table 3: Comparison of critical buckling pressures for perfect circular toroidal shells under uniform external pressure.

a/t	A/a	p_{cr} (MPa)			
		Sobel & Flügge	Wang & Zhang	Galletly & Błachut	Abaqus (S4R) Present study
100	2.0	0.563	0.563	0.545	0.545
100	8.0	0.239	0.222	0.221	0.221
500	2.0	0.0126	0.0128	0.0125	0.0125
500	8.0	0.0052	0.005	0.005	0.00499

3. Parametric study

A wide range of geometric parameters of the circular-elliptical toroidal vessel was systematically selected and considered in this section to investigate the influence of the toroidal cross-sectional height to width ratio, opening ratio, and thickness ratio on the bifurcation and collapse behaviour of the toroidal assemblies, as reported in the following:

3.1. Effects of the toroidal cross-sectional height-to-width ratios
Using the Abaqus finite element code, eigenvalue buckling and nonlinear Riks static analyses were conducted on circular-elliptical toroidal vessels under uniform external pressure with S4R shell models. The b/a ratios are 0.5, 0.75, 1, 2, 3, and 4 as shown with the other geometric parameters and corresponding failure values in Table 4, where the numbers in brackets denote the number of circumferential waves developed at the bifurcation.

Table 4: Bifurcation pressure, p_{bif} and collapse pressure, p_{col} for externally pressurised toroidal vessels with various values of b/a.

b/a	A/a	a/t	$p\,(MPa)$		
			p_{bif}	p_{col}	p_{cr}
0.5	2.0	200	-	0.0601	0.0601
0.75	2.0	200	-	0.0843	0.0843
1.0	2.0	200	0.1068(0)	0.4383	0.1068
2.0	2.0	200	-	0.1848	0.1848
3.0	2.0	200	0.1603(27)	0.2434	0.1603
4.0	2.0	200	0.0918(22)	0.1931	0.0918

In Table 4, it is noticed that for some values of b/a ratios, the pressurised vessels did not fail by asymmetric bifurcation. Interestingly, within this range of values of b/a, a vessel with $b/a = 1$ (which is, of course, a complete circular toroidal vessel) is found to bifurcate with $n = 0$ circumferential waves. This externally pressurised vessel is seen to have a very stable post-buckling state as the final collapse pressure p_{col} of the vessel is over four times higher than the bifurcation buckling pressures of $0.1068MPa$. This is the highest collapse pressure to bifurcation pressure ratio obtained for the various b/a studied.

In the last column of Table 4, one would note that as b/a increases from 0.5, the critical pressure p_{cr} increases steadily until the highest value is attained before reducing steadily. The increase in the values of p_{cr} as b/a increases is seen among the relatively short vessels with characteristic first failure modes that are not asymmetric. For the taller vessels, the values of p_{cr} decrease as b/a increase. The critical failure mode for these tall vessels is asymmetric about the principal axis of revolution of the vessels.
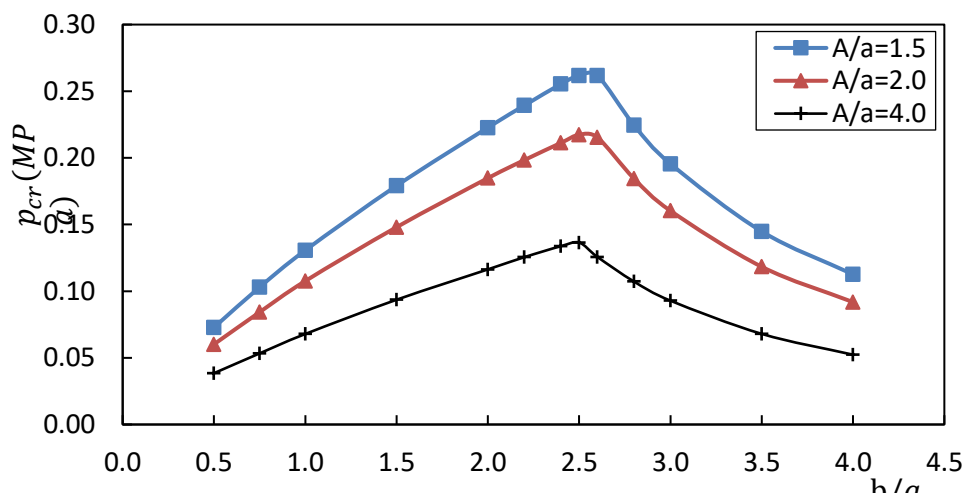

Figure 4: Critical buckling pressure versus b/a ratio for different toroidal opening ratios

To get a clearer picture of the vessels to be called 'short' or 'tall' vessels, changes in b/a were investigated with different values of the toroidal opening ratios A/a. The values of A/a

considered are relatively for compact $(A/a=1.5)$, medium $(A/a=2.0)$ and large diameter $(A/a=4.0)$ geometries of the circular-elliptic toroidal vessel, while the b/a value was varied from 0.5 to 4.0, and the thickness ratio a/t, support conditions applied only to the inner-most equator and material properties remained the same as before. The critical buckling pressures for the various b/a ratios are shown in Figure 4.

For the different values of A/a, results in Figure 4 show that the critical buckling pressure of the vessels increases steadily until a peak value is reached before reducing as b/a increases from 0, as seen before in Table 4. Hence, as far as first buckling pressure is concern, Figure 4 indicates that toroidal vessels of the type under present investigation are stronger (with peak critical buckling values) if the value of b/a is around 2.5 for $a/t=200$. However, as mentioned in Section 4.1, the highest collapse pressure of all b/a ratios studied was obtained for circular toroids $(b/a=1.0)$.

It is also observed that there are distinctly different critical buckling modes corresponding to the toroidal vessels on both sides of the peak pressure value in Figure 4. For $a/t=200$, the critical buckling modes for toroidal geometries with b/a up to 2.5 are axisymmetrical about the global axis of revolution of the toroids with zero circumferential wave number $(n=0)$, while those after $b/a=2.5$ are not symmetrical about the global axis of revolution of the toroids with corresponding circumferential wave number that is always greater than zero $(n>0)$. This transition from buckling mode with $n=0$ to that of $n>0$ is seen not be a function of A/a. Typical examples of these distinctive buckling modes and their corresponding sectional views are depicted in Figure 5 for each of the indicated circular-elliptic toroidal geometries.
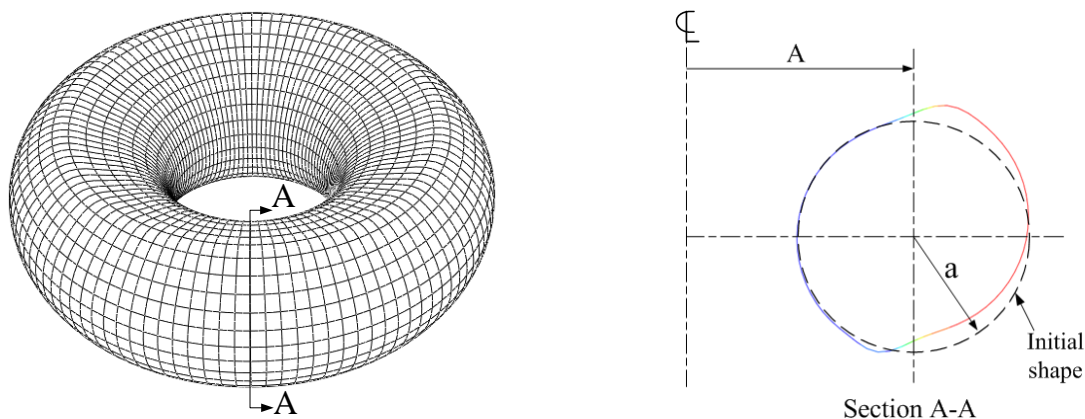

Figure 5(a): View of axisymmetric bifurcation buckling mode for a short toroid with $b/a=1$, $A/a=2$, $a/t=200$, $n=0$, $p_{cr}=0.108MPa$

3.2.Effects of the toroidal opening ratios

The effects of change in toroidal opening ratios on buckling pressures could be seen in Figure 4, where results of critical buckling pressures calculated for different values of A/a are shown. It is observed that the failure pressure of a circular-elliptic toroidal vessel greatly depends on the compactness of the vessel. For the three A/a values, i.e. 1.5, 2, and 4 studied, the critical pressure values of the vessels generally reduce in that order. It shows that higher failure pressures are associated with 'compact' vessels when compared to corresponding vessels with larger opening A/a ratios.
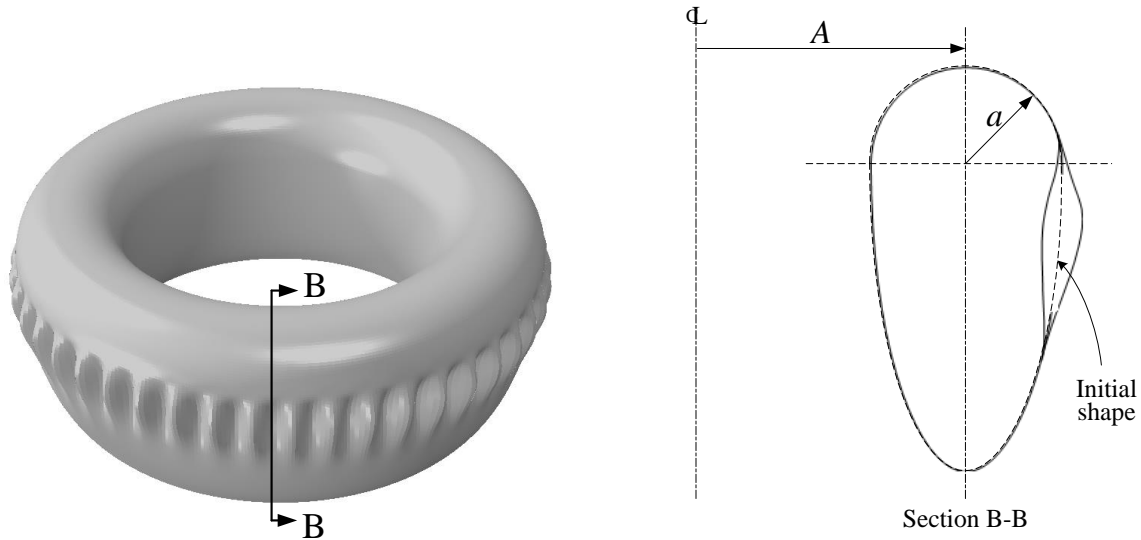
Figure 5(b): View of asymmetric bifurcation buckling mode for a tall toroid with $b/a = 3.0$, $A/a = 4$, $a/t = 200$, $n = 45$, $p_{cr} = 0.093MPa$

The rate at which the buckling pressure changes with A/a was investigated for various circular-elliptic toroidal geometries. Constant values of $b/a = 2$ and $a/t = 200$ were adopted, and the toroidal opening A/a ratio was varied from 1.25 to 16. The vessels were modelled in Abaqus with S4R shell elements by adopting the mesh densities, boundary constraints, and elastic material properties of the previous examples.

Eigenvalue and nonlinear static analyses were conducted on perfect toroidal vessels and the critical pressure values for the different toroidal opening ratios were recorded and plotted in Figure 6. The plot shows that critical pressure value of the pressurised vessels reduces rapidly as the opening ratio A/a increases to 4 approximately, and then steadily until A/a reaches around 9, after which the critical pressure value then reduces slowly, so that the behaviour of the vessel will be identical to that of a long cylindrical shell, as $A/a \to \infty$.
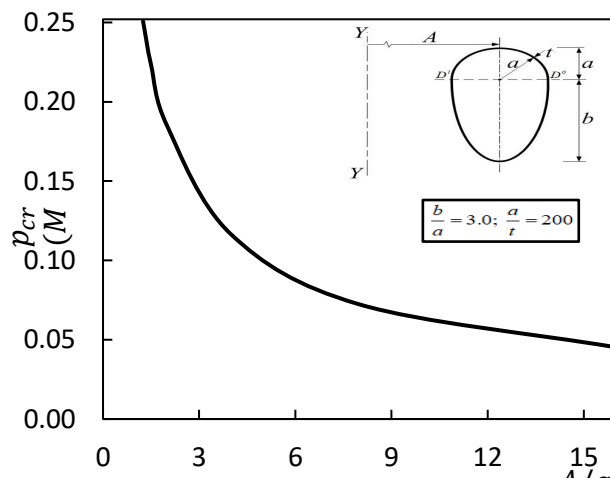

Figure 6: Critical buckling against A/a for toroids with $b/a = 2$, $a/t = 200$

3.3. Effects of wall thickness ratios

The influence of changes in wall thickness on the buckling strength of circular-elliptic toroidal assemblies was investigated with S4R shell models. The eigenvalue and nonlinear Riks analyses in Abaqus were employed in the study. Consistent with the material properties and support conditions as adopted above, toroids with $b/a = 1$, $A/a = 2$ and various thickness ratios were first considered. The load-deflection curves obtained for externally pressurised vessels with values of a/t ranging from 50 to 500 are shown in Figure 7. As before, the reference point for the deflection values was assumed to be the nadir of the vessels.
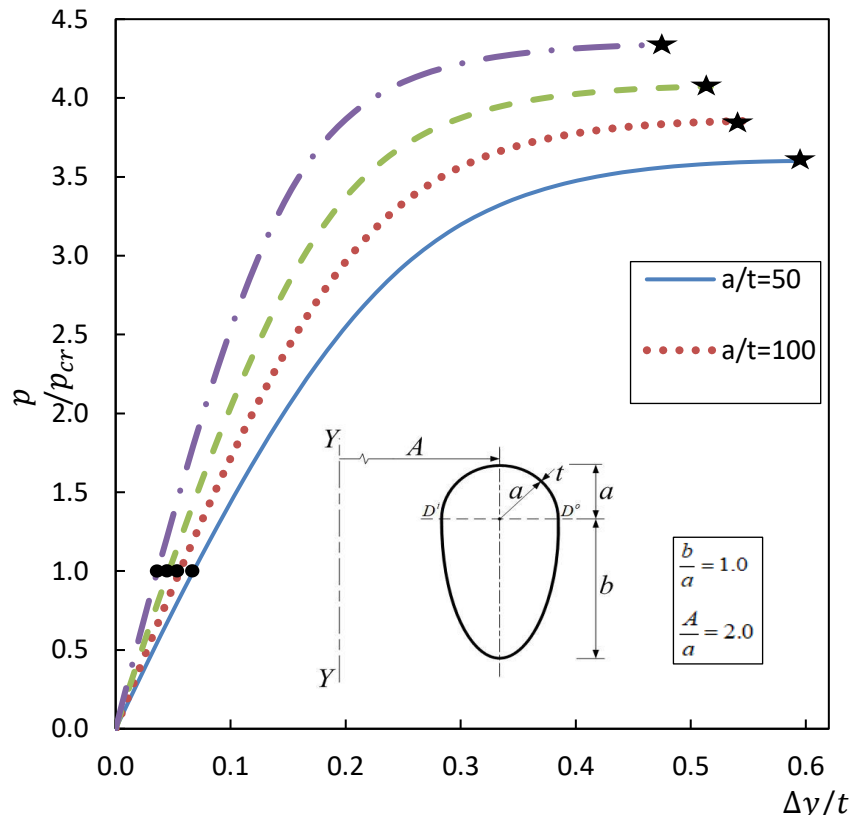

Figure 7: Plot of external pressures against nadir deflection for circular-elliptic toroids with different a/t values.

Table 5: Bifurcation and collapse pressures of externally pressurised circular-elliptical toroids with different a/t values.

b/a	A/a	a/t	$p_{bif}(MPa)$	$p_{col}(MPa)$
1.0	2.0	50	2.7996	10.0810
1.0	2.0	100	0.5470	2.1084
1.0	2.0	200	0.1076	0.4383
1.0	2.0	500	0.0127	0.0549

The position of the bifurcation pressure p_{bif} and the axisymmetric collapse pressure p_{col} are indicated in Figure 7. The magnitudes of these pressure loads are given in Table 5. As expected, it

is seen that both bifurcation and axisymmetric collapse pressures of the toroidal vessel reduce as the thickness ratio a/t increases. That is, as the wall thickness t increases, the failure pressure of the vessel increases.

The rate at which the buckling pressure changes with a/t was also investigated for various circular-elliptic toroidal geometries with three different values of b/a and a single value of $A/a = 2.0$. The toroidal thickness ratio a/t was varied from 50 to 500. The idealization employed in the modelling of the perfect vessels, including the support conditions and material properties are the same as above. Eigenvalue and nonlinear static analyses were used for the calculation of pressure values in Abaqus, and the critical pressure values for the different values of b/a obtained are plotted against the toroidal thickness ratio a/t in Figure 8. The plot shows that critical pressure values of the pressurised vessels reduce spontaneously as a/t increases to 140 approximately, and then reduces slowly afterwards.
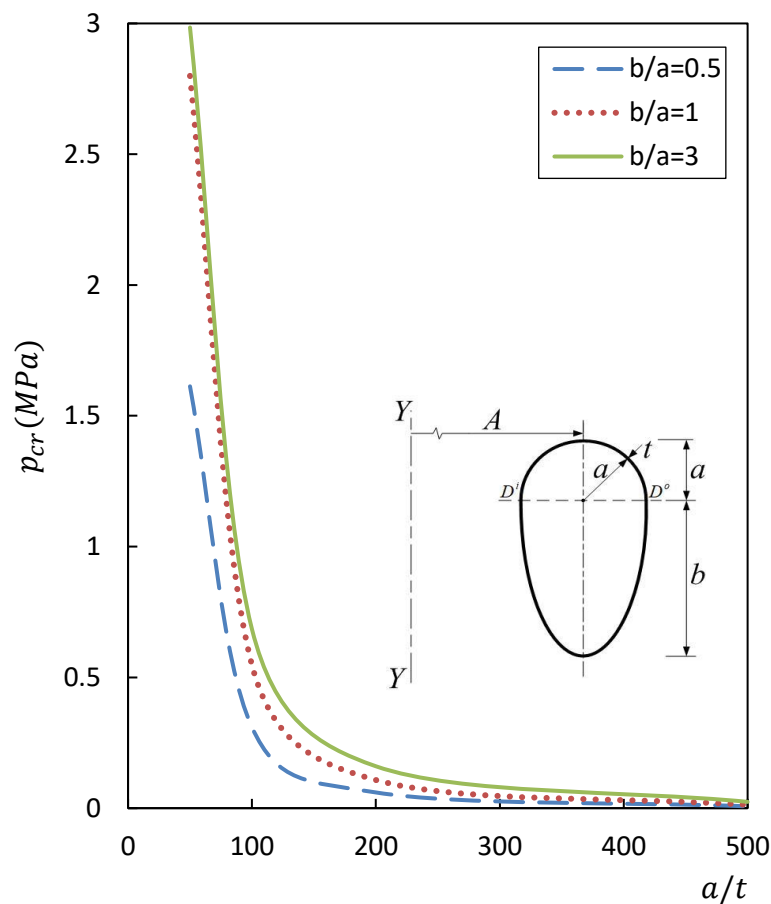

Figure 8: Plot of external pressures versus thickness ratios a/t for toroids with different b/a values

4. Conclusion

The buckling behaviour of a novel toroidal vessel with circular-elliptical cross-section under external pressure loading has been numerically studied in this paper, including the buckling response of the vessel due to changes in the cross-sectional geometrical parameters. It is seen that the vessel generally has a stable post-buckling behaviour and may, therefore, be able to resist further load beyond the elastic bifurcation loads. The buckling shape or weakest zone where the buckling

normally starts from is a function of b/a. For $b/a \gg 1$, buckling initiates non-axisymmetrically in the elliptic segment near the meeting edges of the vessels before nonlinear buckling 'snap-through' occurs at a larger collapse pressure load, while toroidal vessels with smaller b/a buckle symmetrically with $n = 0$.

In all the different b/a studied, circular toroids ($b = a$) are found to have the highest collapse pressure to bifurcation pressure ratio of up to 4. It is also observed that, as b/a increases, the critical pressure p_{cr} increases steadily until the highest value is attained before reducing steadily. The increase in the values of p_{cr} as b/a increases is seen among the relatively short vessels with characteristic first failure modes that are not asymmetric. For the taller vessels, the values of p_{cr} decrease as b/a increase. The critical failure mode for these tall vessels is asymmetric about the principal axis of revolution of the circular-elliptic toroidal vessels. For toroids with $a/t = 200$, the critical buckling modes for toroidal geometries with b/a up to 2.5 are axisymmetric about the global axis of revolution of the toroids with zero circumferential wave number $(n = 0)$, while those after $b/a = 2.5$ are not symmetrical about the global axis of revolution of the toroids with corresponding circumferential wave number that is always greater than zero $(n > 0)$. This transition from buckling mode with $n = 0$ to that of $n > 0$ is seen not be a function of A/a.

References

[1] Sun, B., (2020): On symmetrical deformation of toroidal shell with circular cross-section. *Xi'an University of Architecture and Technology*, Xi'an, China. Technical paper.

[2] Galletly, G.D., Blachut, J., (1995): Stability of complete circular and non-circular toroidal shells. *Proc.Inst.Mech.Engrs.* Vol 209 (c) pp 245-255.

[3] Jasion, P., Magnucki, K. (2012): Elastic buckling of horizontal barreled shells filled with liquid: Numerical analysis. *Thin-Walled Structures,* Vol. 52, pp 117-125.

[4] Chan G.C.M., Tooth, A.S., Spence, J. (1998): A study of the buckling behaviour of horizontal saddle supported vessels. *Thin-Walled Structures*, Vol. 30, pp 3-22.

[5] Galletly, G.D., (1998): Elastic Buckling of Complete Toroidal Shells of Elliptical Cross-Section Subjected to uniform Internal Pressure. *Thin-Walled Structures*, Vol. 30 pp 23-34.

[6] Bushnell, D., (1976): BOSOR 5-program for buckling of elastic-plastic complex shells of revolution including large deflections and creep. *Computers and Structures,* Vol 6, pp 211- 239.

[7] Combescure, A., (1986): Static and dynamic buckling of large thin shells. *Nuclear Engineering Design.* Vol 92. pp 207-224.

[8] Combescure, A., Galletly, G.D. (1999): Plastic buckling of complete toroidal shells of elliptical cross-section subjected to internal pressure. *Thin-Walled structures*, Vol. 34, pp 135-146.

[9] [9] Blachut, J., Smith, P. (2008): Buckling of multi-segment underwater pressure hull. *Ocean Engineering.* Vol.35 pp 247-260.

[10] Enoma, N., Zingoni, A. (2020): Buckling of an externally pressurized toroidal shell of revolution with a doubly-symmetric parabolic-ogival cross-section. *International Journal of Pressure Vessels and Piping*. Vol 183, pp 104106.

[11] Crisfield, M.A. (1981): A fast incremental/ iterative solutions procedure that handles "snap-through". *Computers & Structures* Vol. 13 (1-3), pp 55-62.

[12] Sobel, L.H., Flugge, W. (1967): Stability of toroidal shells under uniform external pressure. *AIAA Journal*. Vol. 5 pp 425-431.

[13] Zhang, H.Q., Wang, M. (1991): *The mathematical theory of finite elements*. Science press, Beijing